

## Letters

## Quantifying the heat affected zone in laser scribing of thin film solar cells

Tizian Bucher<sup>a,\*</sup>, Grant Brandal<sup>b</sup>, Hongqiang Chen<sup>c</sup>, Y. Lawrence Yao<sup>b</sup><sup>a</sup> Advanced Manufacturing Laboratory, Department of Mechanical Engineering, Columbia University, 500 West 120th Street, Room 220, New York, NY 10027, United States<sup>b</sup> Advanced Manufacturing Laboratory, Department of Mechanical Engineering, Columbia University, New York, NY 10027, United States<sup>c</sup> GE Global Research, Niskayuna, NY 12309, United States

## ARTICLE INFO

## Article history:

Received 19 January 2017

Received in revised form 3 May 2017

Accepted 7 May 2017

Available online 12 May 2017

## Keywords:

Laser scribing

Thin film solar cell

Heat affected zone

Kelvin probe force microscopy

## ABSTRACT

Laser scribing is a method for partitioning thin film solar panels into a series of mini-modules. While glass-side laser scribing is meant to be a thermally-induced mechanical material removal method, significant thermal damage may occur if the process is not properly designed. No approach has been developed yet to conveniently measure the size of the heat affected zone. Kelvin probe force microscopy was proposed and used to measure the heat affected zone via changes in the work function of the material. It was found that mechanically dominated material removal yields the smallest HAZ while also achieving a satisfactory electrical isolation.

© 2017 Society of Manufacturing Engineers (SME). Published by Elsevier Ltd. All rights reserved.

## 1. Introduction

Multilayer thin-film solar cells have gained increased popularity since they can readily be manufactured on a large scale using inexpensive and flexible substrates. In order to obtain high-voltage and low-photocurrent devices and thereby reduce resistive losses, the solar cells need to be scribed into an array of mini-modules that are connected in series. Glass-side laser scribing is a scribing method that allows for a mechanical material removal through thermally-induced stresses [1]. The multilayers are scribed one layer at a time. The first one is the P1 scribe, in which the back contact transparent conducting oxide (TCO) layer is removed to create an electrical isolation between adjacent mini-modules. If the P1 scribe fails to fully remove the TCO layer, a shunt current can form between adjacent mini-modules, which causes a dramatic drop in the solar panel efficiency [1,2]. Shunt currents can generally be reduced by using higher laser fluences and thus increasing the material removal. However, while an increased laser fluence alleviates problems related to shunt losses, it generates extended heat affected zones (HAZ) adjacent to the laser scribe. Inside the HAZ high temperatures are reached, causing material dopants to precipitate out of TCO at elevated temperatures, therefore diminishing the beneficial impact of the doped agent on the material [3,4]. In this study, fluorine-doped SnO<sub>2</sub> was employed as a TCO layer, where the fluorine dopant served to increase the electrical conductivity of the material. With the

fluorine precipitating out of SnO<sub>2</sub> at elevated temperatures, the electrical conductivity of the material drops significantly, increasing the serial losses of the solar cell.

Many researchers have identified concerns related to thermal damage [5–7], however, no approach has been developed to conveniently measure the size of the heat affected zone. In this study, a new approach is presented to measure the size of the HAZ using Kelvin probe force microscopy (KPFM), which helps maximize the effectiveness of the scribing process.

## 2. Theory

A material's work function is the minimum amount of energy required to remove an electron from the Fermi level, and plays an important role in the performance of solar cells. When designing solar cells the materials are chosen so that the differences in work function at dissimilar interfaces can help optimize the performance. At the interface between the TCO and the photovoltaic layer the work function mismatch creates a diode, where various levels of doping can be used to alter the photovoltaic layer's work function. Proper choice of materials can then create a built in electric field that promotes charge transfer. But deviation from the prescribed work function values causes band bending across a particular length from the interface and potentially results in a barrier to current flow of the electrons [8]. This effective screening length can be expressed as

$$L_s = 2 \sqrt{\frac{\epsilon_0 \epsilon_r kT}{2q^2 |Q_{tot}|}} * \sqrt{\frac{q|\Delta W F|}{kT}} \quad (1)$$

\* Corresponding author.

E-mail address: [tb2430@columbia.edu](mailto:tb2430@columbia.edu) (T. Bucher).

where  $\epsilon_0$  is the permittivity of free space,  $\epsilon_r$  is the dielectric constant,  $k$  is Boltzmann's constant,  $T$  is temperature,  $q$  is the elementary charge,  $Q_{tot}$  is the spatial charge density across the buffer layer, and  $\Delta WF$  is the difference in work function of the buffer layer and the TCO. Thus, any decreases in the work function of the TCO layer from heat affected zones of P1 laser scribing will cause increases to  $\Delta WF$ , leading to increases in the effective screening length and decreases in device performance. For TCO/n-Si solar cells [9] and indium oxide TCO layers [10], for instance, increases in fill factors and decreases in efficiencies could be traced back to increases in  $\Delta WF$ .

### 3. Material and methods

Glass side P1 scribing was performed on fluorine-doped tin dioxide ( $\text{SnO}_2:\text{F}$ ) thin film samples deposited on 3.2 mm thick soda-lime glass substrates. The  $\text{SnO}_2:\text{F}$  layers had a thickness of 400 nm, determined via ellipsometry. To limit the amount of removed material that redeposited onto the substrate, the samples were suspended with the  $\text{SnO}_2:\text{F}$  facing down, and the laser incident from above. Scribing was performed in straight lines to create four sides of a square. To counteract the effects of the motion stage accelerating to the desired velocity, each side of the square was extended, forming an overall shape similar to a hashtag. Thus, electrical isolation was created between the inside and the outside of the squares for measuring the resistance across the scribe. The samples were rinsed with acetone and allowed to air dry prior to scribing.

Two different scanning speeds were investigated, 15 mm/s and 50 mm/s. As the spot size was 20  $\mu\text{m}$ , these speeds correspond to roughly 90% and 75% overlap. A redENERGY G4 H-Type fiber laser system from SPI Lasers was implemented at a wavelength of 1064 nm and repetition rate of 10 kHz. Pulse energies ranged from 12.5 to 40  $\mu\text{J}$ . Two Aerotech ALS130-50 mechanical bearing linear motor stages performed sample manipulation. Kelvin probe force microscopy (KPFM) was performed on a Bruker Dimension FastScan AFM in PeakForce KPFM mode, with PFQNE-AL probes. Resistance measurements were made with a Fluke 87 III True RMS Digital Multimeter.

### 4. Results and discussion

At low laser fluences the shunt resistance across the P1 scribe increases with increasing laser fluence, as shown in Fig. 1. At 20  $\mu\text{J}$  (for 15 mm/s) and 17.5  $\mu\text{J}$  (for 50 mm/s), the material removal is complete and the shunt resistance reaches a high value at around  $10^7 \Omega$  at both scan speeds. Beyond these laser fluences, the shunt resistance remains almost constant, and no further improvement in the electrical isolation is achieved. Therefore, from an electrical isolation standpoint, the laser fluence may be chosen arbitrarily high as long as it is not smaller than the aforementioned threshold.

The analysis of the heat affected zones shows that the above result is not sufficient to provide a good scribe quality. The HAZ was determined using Kelvin probe force microscopy by measuring the work function across the scribe. Fig. 2 shows a two dimensional scan across one of the walls of the scribe, where the left side of the image is in the center of the scribe and the right hand side is outside of the scribe. The units of the data, contact potential difference, is the difference in work function  $\Delta WF$  of the KPFM probe and the workpiece. To calculate the work function, one must simply subtract this potential from the work function of the probe, which in our case  $\varphi_{tip} = 4.4 \text{ eV}$ . Moving from left to right in the image, a clear minimum in work function at the bottom of the scribe is seen, with a transition region in the center of the figure

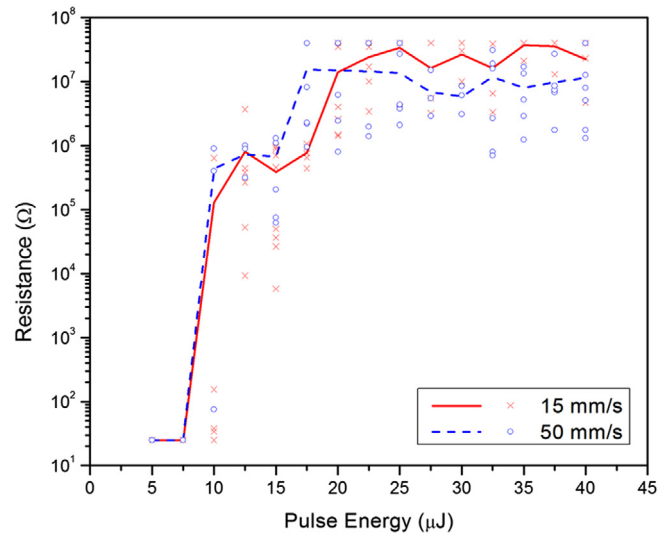


Fig. 1. Shunt resistance measured across P1 scribes. Complete material removal and a maximum attainable electrical isolation is obtained starting at 20  $\mu\text{J}$  (for 15 mm/s) and 17.5  $\mu\text{J}$  (for 50 mm/s).

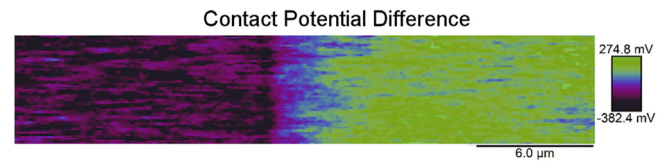


Fig. 2. Contact potential difference 2D scan across a P1 scribe performed at 22.5  $\mu\text{J}$  and 50 mm/s. Only one of the scribe walls is shown, as the other wall is the same by symmetry. The contact potential difference indicates changes in work function.

before reaching the high values of the untreated material outside of the scribe.

From Fig. 2, the work function difference  $\Delta WF$  was extracted along a horizontal line (Fig. 3b) and plotted together with the topography along the same path (Fig. 3a). The region between the dotted lines shows the scribe wall width (Fig. 3a) and the corresponding heat affected zone (Fig. 3b), whereby the HAZ extends far beyond the scribe wall width. The HAZ can be identified in this manner since the gradual increase in the work function also indicates some residual material, while the change at a dissimilar interface would be more abrupt. This HAZ measurement was performed on a range of pulse energies and two different scribing speeds, as presented in Fig. 4.

Rather than having a simple linear increase in HAZ with increasing pulse energies, the profiles in Fig. 4 have a “V” shape that is attributed to the competition between mechanical and thermal removal mechanisms that are thoroughly discussed by Wang et al. [6] and Brandal et al. [7]. At both low and high laser fluences thermal material removal mechanisms dominate that causes a large HAZ. Mid-range laser fluences between 20 and 22.5  $\mu\text{J}$ , on the other hand, promote a mechanically-dominated removal with a smaller HAZ. Therefore, KPFM could successfully be used to identify the size of the HAZ, yielding results that are in agreement with previous qualitative results published in [6,7]. Moreover, the combination of the shunt resistance and HAZ measurements indicate that increasing the laser fluence beyond mid-range (20–22.5  $\mu\text{J}$ ) does not improve the electrical isolation but increases the HAZ.

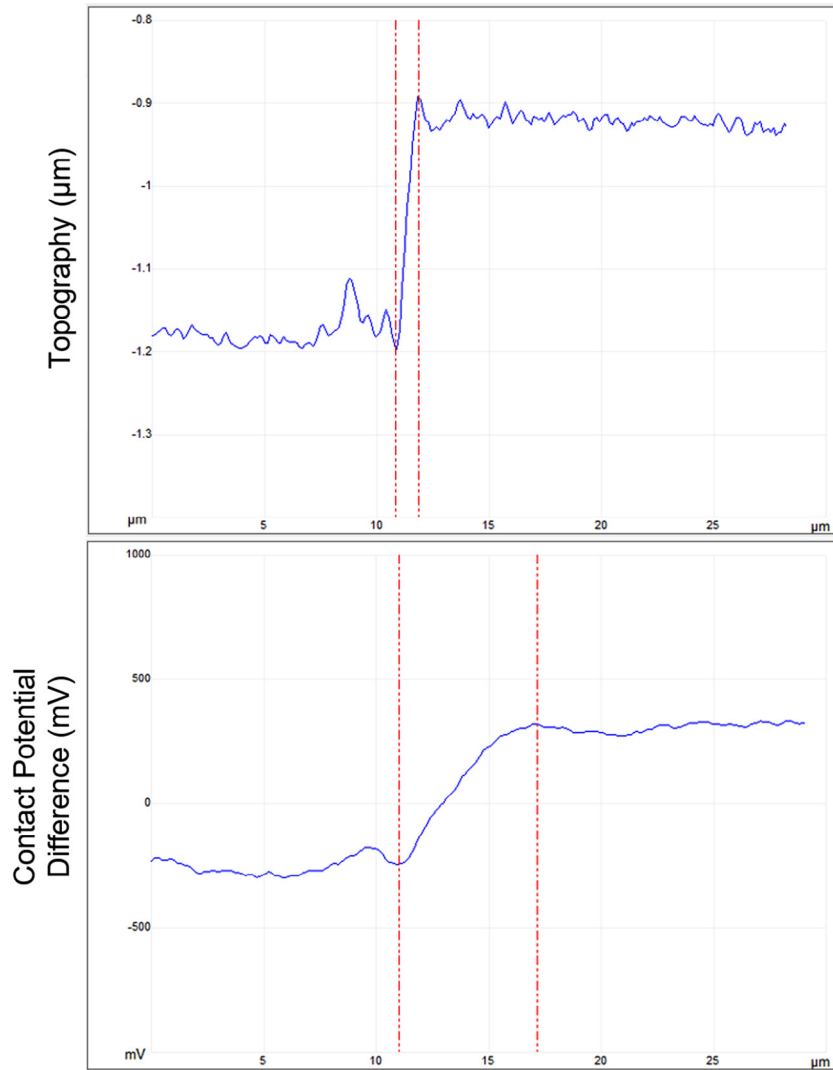


Fig. 3. (a) Topography scan line profile of the sample in Fig. 2 using an AFM; (b) presents the contact potential difference along this line, showing a HAZ that extends beyond the wall of the scribe.

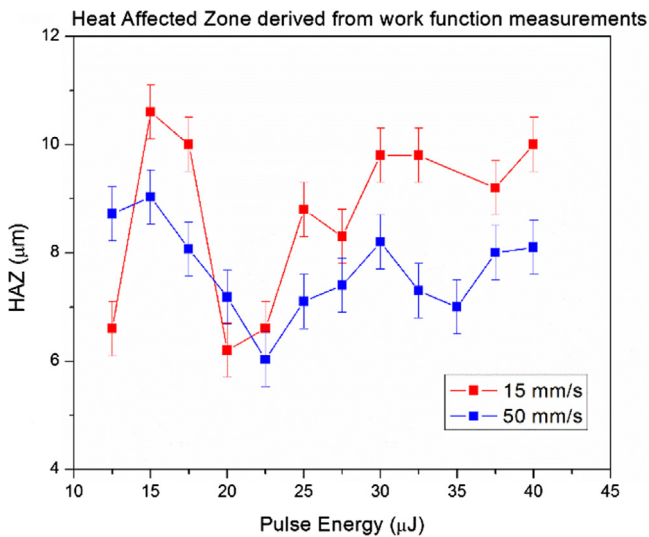


Fig. 4. Extent of the heat affected zone over a range of incident laser pulse energies, 3 measurements were performed for each condition. Mid-range fluences between 20 and 22.5 μJ correspond to thermally induced mechanical fracture becoming the dominant removal mechanism.

### 5. Conclusions

It is shown that Kelvin probe force microscopy is an accurate method to determine the extent of the heat affected zone by measuring changes in the work function. The results obtained are in agreement with qualitative results that were reported previously. Together with the shunt resistance measurements, the results indicate that mid-range laser fluences yield the smallest HAZ while also generating a satisfactory electrical isolation. Therefore, KPFM can be used as an important tool to determine the optimum processing conditions of P1 scribing of thin film solar cells with an SnO<sub>2</sub>:F back contact layer. The approach can be readily applied to other types of solar cells, and even be used to determine the optimum processing window for other scribing types such as P2 and P3 scribes.

### Acknowledgment

This work is supported by GOALI grant CMMI-1333241 from NSF. Support from Columbia University and GE Global Research is also gratefully acknowledged.

## References

- [1] Compaan AD, Matulionis I, Nakade S. Laser scribing of polycrystalline thin films. *Opt Lasers Eng* 2000;34(1):15–45.
- [2] Gečys P, Račiukaitis G, Miltenis E, Braun A, Ragnow S. Scribing of thin-film solar cells with picosecond laser pulses. *Phys Procedia* 2011;12:141–8.
- [3] Pavelko RG, Vasiliev AA, Vilanova X. Long-term stability of SnO<sub>2</sub> gas sensors: the role of impurities. *IEEE Sensors* 2008:815–8.
- [4] Melghit K, Bouziane K. Low-temperature preparation and magnetic properties of V-Doped SnO<sub>2</sub> nanoparticles. *J Am Ceram Soc* 2007;90(8):2420–3.
- [5] Wang H, Hsu S, Tan H, Yao YL, Chen H, Azer MN. Predictive modeling for glass-side laser scribing of thin film photovoltaic cells. *J Manuf Sci Eng* 2013;135:051004.
- [6] Wang H, Chen H, Yao YL. Removal mechanism and defect characterization for glass-side laser scribing of CdTe/CdS multilayer in solar cells. *J Manuf Sci Eng* 2015;137(6):061006.
- [7] Brandal G, Ardelean J, O'Gara S, Chen H, Yao YL. Comparative Study of Laser Scribing of SnO<sub>2</sub>: F Thin Films using Gaussian and Top-Hat Beams. *ICALEO 2015, Atlanta*; M603.
- [8] Klein A, Christoph K. Transparent conducting oxides for photovoltaics: manipulation of fermi level, work function and energy band alignment. *Mat* 2010;3(11):4892–914.
- [9] Chen A, Zhu K. Effects of TCO work function on the performance of TCO/n-Si hetero-junction solar cells. *Sol Energy* 2014;107:195–201.
- [10] Centurioni E, Iencinella D. Role of front contact work function on amorphous silicon/crystalline silicon heterojunction solar cell performance. *IEEE Electron Device Lett* 2003;24(3):177–9.